The Acoustics of the Alto Horn and Euphonium

Annelise Roti Roti
Engineering Physics Department, University of Wisconsin – Platteville

ABSTRACT

Near-field acoustic holography was used to characterize properties of the air column at the bell end of a Besson Euphonium and a CG Conn E♭ Alto Horn; harmonic analysis was used to understand what causes the timbres that musicians call “bright” and “dark”. Circuit analysis was then used to begin the modelling of the acoustic system electrically.

It was shown by the data that what musicians call “bright” is correlated with a high number of harmonics, and “dark” correlated with few harmonics. The holography scans showed that a 180° phase shift occurs at the bell end between each resonant frequency, and that the pressure and particle velocity of the air column are not constant across the area of the bell. Finally, a lumped-parameter electrical circuit model capable of predicting a resonance, given all measured parameters, was developed.

I. Background and Introduction

A. The E♭ Alto Horn

The E♭ Alto Horn, hereafter to be referenced as “Alto Horn”, is a brass instrument whose playing range is analogous to that of the French Horn (deemed simply “Horn” in Europe). The Alto Horn is brighter in tone than a French Horn or a Euphonium, and its primary use is in British brass bands. A 100-year-old CG Conn Alto Horn is used here; it is analyzed in this investigation due to its availability and close relation to the Euphonium.

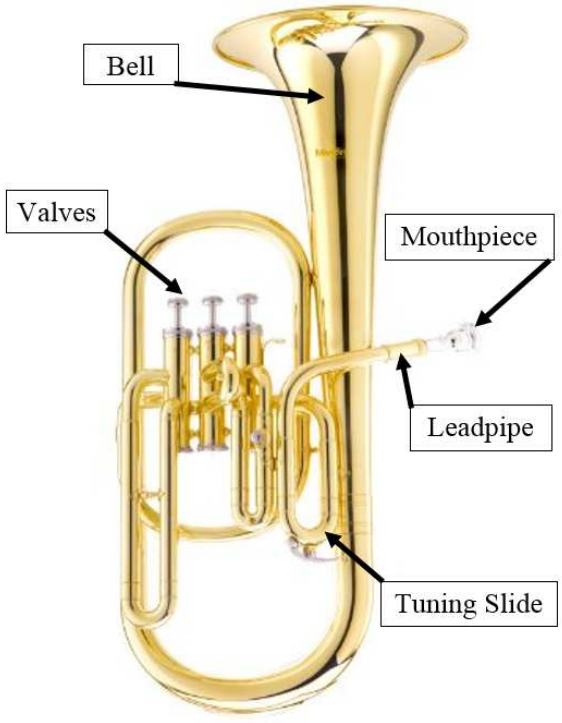

Figure 1 Mendini E♭ Alto Horn, similar to the CG Conn used in testing. Photo courtesy of Amazon.com.

B. The Euphonium

The Euphonium is a brass instrument which plays in the tenor to baritone range. On high-end intermediate or professional models, a professional performer has a range from approximately E_1 to E_5. The euphonium has a sweet-sounding tone and is aptly named, as ‘euphonos’ comes from the Greek root meaning “well-sounding”[1]. Figures 1 and 2 show the construction of both instruments.

C. Playing Mechanism

Both tested instruments are piston-valve "lip-reed" instruments; they are played using a cup-shaped mouthpiece that is inserted into the leadpipe of the instrument. Sound is produced by a player exciting the air column by "buzzing", or vibrating, their lips inside the mouthpiece.

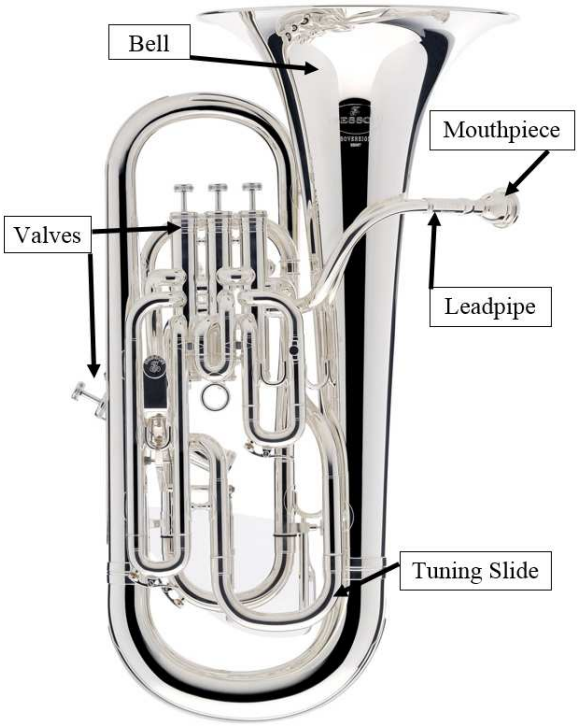

Figure 2 "3&1" compensating Sovereign Model Euphonium manufactured by Besson. Image courtesy of www.bettermusic.com

Valves allow the player to vary the playable pitches by depressing one or more at a time. On euphoniums like the Besson, there are three valves at the top of the instrument and one on the side. This is called a "3&1 compensating" valve array, indicating that the fourth valve can be used instead of the "3+1" fingering and allows the player access to a full octave below E_2. Other valve arrays include "4-valve inline", where the four valves are arranged on the top of the instrument, and the "3-valve" array.

When a brass instrument is played, the sound waves propagate through the tubing, creating a tangible plane of dense air that exists either inside the bell or just above the plane of the bell, and covers the whole bell face. Brass musicians call this a 'reflection point', and it is most prevalent in low-voice instruments such as the euphonium and tuba. Its placement within the bell is frequency dependent, and its perceived 'density' is intensity dependent, as can be determined by brief experimentation.

D. Specific Acoustic Impedance

Specific acoustic impedance is a complex quantity that describes the resistance of the medium to allow a sound wave to propagate through it, and is defined as:

$$\tilde{z} = \frac{\tilde{p}}{\tilde{u}} \left(\frac{Pascals*sec}{m}\right) \quad (1)$$

Where $\tilde{z}$ is the complex impedance in Rayls (or acoustic Ohms, Ω_a), $\tilde{p}$ the complex pressure in Pascals, and $\tilde{u}$ the complex particle velocity in meters per second. The tilde represents the fully complex nature of the quantities, which can described, for a harmonic sound field, as:

$$\tilde{p}(\vec{r}, t) = \tilde{p}(\vec{r}, \omega) * e^{i\omega t} \quad (2)$$

and

$$\tilde{u}(\vec{r}, t) = \tilde{u}(\vec{r}, \omega) * e^{i\omega t} \quad (3)$$

Fourier analysis states that three quantities are necessary to fully re-create a periodic waveform: frequency, amplitude, and phase. Recording this information allows us to analyze playable notes as well as the phase relationship of those notes within the instrument.

Playable notes occur at resonances, where $\tilde{z}$ is at a maximum; each valve combination changes which resonances exist. A frequency-dependent impedance mismatch between the bell and free air causes sound waves to be reflected back to the mouthpiece. At a resonant frequency, these waves interfere constructively at the mouthpiece with waves generated by the lips, reinforcing the physical buzzing and amplifying the sound.

E. Harmonics

Harmonics are the pitches that are audible other than and simultaneously with the fundamental frequency. In brass instruments, a harmonic's frequency, f_n is an integer multiple of the fundamental frequency, f_1, such that $f_n = nf_1$ for n=1, 2, 3, etc. These harmonics follow the resonant pattern of the diatonic scale[2], so if a player sounded B♭2, a listener would also hear B♭3, F4, B♭4, D5, F5, G5, and B♭5, though the amplitudes of those harmonics are significantly diminished.

F. Electrical Analogs for Instruments

As mentioned above, the frequency dependent impedance mismatch at the bell causes some sound waves to be reflected back into the instrument while allowing others to propagate into space. At frequencies of playable notes, the phase of the reflected wave is such that it sets up a standing wave in the instrument, creating a resonance.

Brass instruments have electrical analogs for each part of their acoustic system. The player's lips act as a function generator, and the mouthpiece gives a high input resistance. The volume of the mouthpiece acts as a capacitance, the tubing an inductance, and the loss of energy to heat acts along the tubing of the instrument as a resistance[3]. The free air outside of the instrument, then, acts as a load resistance with a value of $415\Omega_a$.

II. Methods

Three tests were performed on each instrument: an audio harmonic analysis to examine harmonic content, a frequency scan to determine resonant frequencies, and a set of XY-planar scans at the bell to examine the characteristics of the sound field just above the plane of the bell. After these tests were complete, a lumped-parameter circuit model of the brass instruments was developed using NI Multisim, a circuit editor and simulation program.

A. Harmonic Analysis

Using a Behringer ECM8000 electret condenser omni-directional reference microphone and a Marantz PMD-671 24-bit digital recorder, various notes were recorded on each instrument.

E♭3, B♭3, E♭4, and G4 were recorded first on the Alto Horn with its proper mouthpiece, and then with a Bach 7C trumpet mouthpiece for data consistency since a modified 7C trumpet mouthpiece would be used in the next two tests. B♭2, F3, D4, and F4 were recorded using an SM4M Denis Wick mouthpiece on the Euphonium, while B♭1, B♭2, F3, B♭3, and D4 were recorded with a plastic 5G Kelly mouthpiece.

After the notes from each instrument were recorded, the .wav files were analyzed using the MATLAB program 'Wav_analysis.m' written by Joe Yasi[4]. The waveforms were clipped to a time frame over which their waveform was stable, and the graphs produced contained information regarding harmonic frequency, amplitude, and phase.

B. Frequency Scan

Using results from the harmonic analysis, an appropriate range of frequencies was scanned to determine a more precise value for each harmonic. For both instruments, this involved setting the instrument up horizontally on a table and placing a pressure and particle velocity ($\tilde{p}\tilde{u}$) microphone pair at the mouthpiece and in the center of the bell, as shown in Figure 3. A foam wall was set up across the room to dampen any potential standing waves that could possibly contaminate the data. These contaminating waves are more than 20dB below the amplitude of the measured waves and arise from the fact that the lab is not an anechoic room.

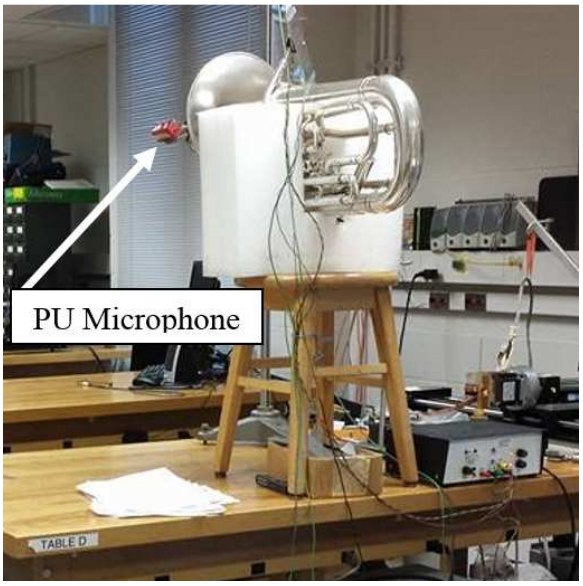

Figure 3 The Euphonium in frequency scanning set-up. The bell is set perpendicular to a level table, and the $\tilde{p}\tilde{u}$ microphone is set on a ring stand to be in the center of the bell. A stacked wall of foam ten feet across the room acts to dampen any possible standing waves.

Both instruments were excited with a piezoelectric transducer disk mounted to a modified mouthpiece. The mouthpiece had three holes drilled in it: one to fit a modified Knowles Electronics EK-23132 omnidirectional microphone, one for a Knowles Electronics FG-23329 omnidirectional condenser electret pressure microphone, and a third for a screw. The screw attaches the mouthpiece to an aluminum strip to support the microphone housings, as shown in Figure 4.

A piezoelectric disk transducer was secured to the rim of the mouthpiece using cyanoacrylate glue. This transducer mechanically models the vibration of a player's lips at a single frequency when an AC voltage is applied across it. Apiezon sealing compound was used to seal off any remaining air leaks after both $\tilde{p}$ and $\tilde{u}$ microphones were inserted into the mouthpiece. The outputs of the custom-built microphone preamplifier were input to four Stanford Research SRS-830 dual-channel Lock-in Amplifiers (LIAs) for data acquisition.

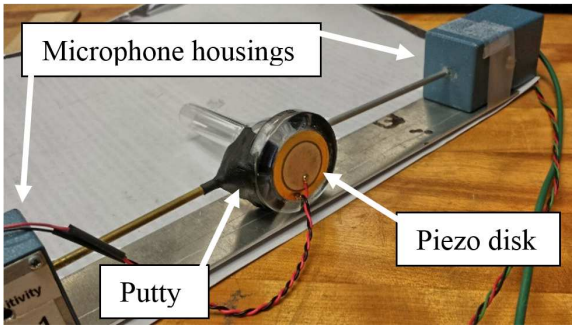

Figure 4 Kelly 5G mouthpiece, modified to host pressure and particle velocity microphones, a piezoelectric transducer disk, and an aluminum strip. Apiezon putty is used to seal any air leaks.

Measurements were taken over a range of 29.5-2030.5Hz in 1Hz steps, and the data were analyzed using a MATLAB program, 'PUsound_Analysis.m', written by Dr. Errede. This analysis computes values for the complex $\tilde{p}$, $\tilde{u}$, $\tilde{z}$, and other acoustic quantities, at both the mouthpiece and the bell. Graphs of each quantity as a function of frequency are produced. The $|\tilde{z}|$-maximum graphs show the frequency at which the resonance occurs, as well as how easily a note can be played sharp or flat based on the width of the resonance. Complex plane graphs show how the phase changes over frequency.

C. XY-Planar Scans

In this investigation, near-field acoustic holography was used to determine the characteristics of the air column 1cm above the bell of each instrument. X- and Y-translation stages run by 1.8° stepper motors, as shown in Figure 5, were used to scan a square area above the bell of each instrument with a PU microphone pair. The Alto Horn was scanned with an area ±15.5cm from the origin in both the x- and y-directions in 1cm steps, while the Euphonium was scanned in the same fashion with an area ±16.5cm from the origin. Pressure and particle velocity were measured at specific mode-locked resonant frequencies at consecutive (x,y) points across the plane of the bell as well as within the mouthpiece[5]. These frequencies drift within one or two Hertz over the course of the scan due to ambient pressure and temperature fluctuations.

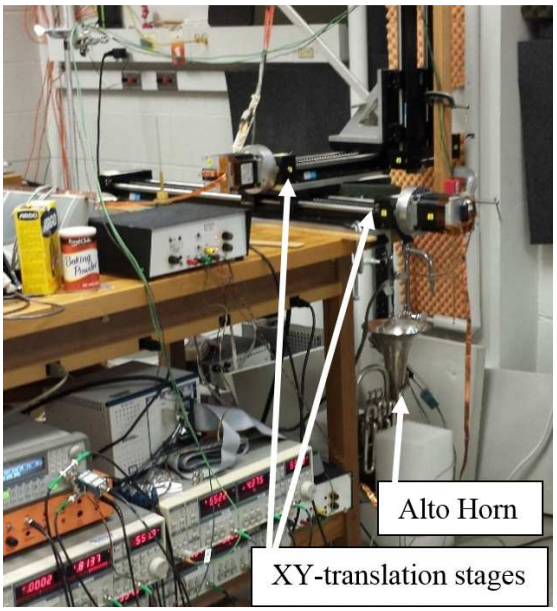

Figure 5 Alto Horn in the bell scan stage. The XY-translations stages are run by stepper motors that have the precision to rotate their crankshafts as little as 1.8° at a time.

Using $\tilde{p}\tilde{u}$ microphone pairs in both the mouthpiece and bell allows the calculation of phase differences over the entire instrument. This aids the analysis of phase-sensitive data and the development of a valid electrical model.

Data from each scan were collected by four LIAs that house a total of eight Analog-Digital Converters (ADCs)[6]. The data were then read into a data acquisition (DAQ) program developed by Dr. Errede and Nicolas D'Anna[7].

The data as collected from the LIAs were analyzed using a MATLAB program, 'Modal_Vibe_Analysis.m', written by Dr. Errede. This program produces over 400 figures that depict various acoustical quantities at both the bell and mouthpiece as a function of x and y. These include real and imaginary components of: pressure, particle displacement/velocity/acceleration, and specific acoustic impedance. They also show raw data and bell vs. mouthpiece phase difference between quantities.

D. Circuit Modeling

The bell of the instrument is modeled as an acoustic transformer with a turns ratio equal to the ratio of areas between the bell and the back bore of the mouthpiece. The capacitance and inductance of the circuit are assumed to be frequency dependent, and thus the equation

$$f_0 = \frac{1}{2\pi\sqrt{LC}} \tag{4}$$

was used to determine the product LC, where f_0 is the frequency.

A large input resistance causes the circuit to be driven at nearly constant current, and this resistance is larger than the combined resistance of the rest of the circuit. The instrument's tubing is modeled as a resistor in series with an inductor; its intrinsic resistive value is chosen arbitrarily to approximate the width of the known resonance peaks. These parameters, when input together, predict a resonant frequency.

III. Results and Discussion

A. Harmonic Analysis

1. The Alto Horn

The harmonic content of the Alto Horn shows a musically bright tone, especially when compared to that of the Euphonium. This timbre is correlated with the number of harmonics that exist when a note is played.

Figures 6-9 show the harmonic content of E♭3, B♭3, E♭4, and G4, respectively, as played with the Alto Horn mouthpiece. These waterfall plots show that the number of audible harmonics decreases with higher frequency, and the timbre becomes musically darker as the player reaches the upper range of the instrument.

These data were recorded using the proper mouthpiece for the instrument. Data recorded with a 7C trumpet mouthpiece, which is much shallower than a real Alto Horn mouthpiece, showed more audible harmonics, indicating a correlation between mouthpiece depth and perceived brightness of timbre.

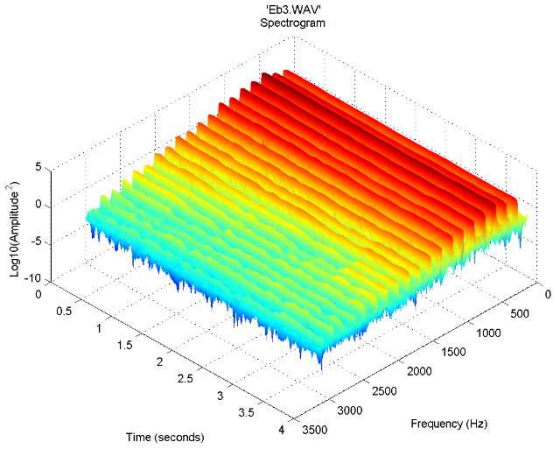

Figure 6 E♭3 is the lowest playable note that will produce a good musical tone on the Alto Horn. It shows nine strong harmonics, indicated by the red peaks.

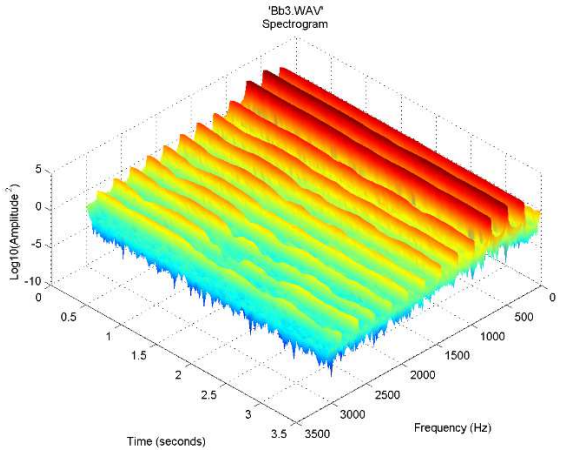

Figure 7 B♭3 is a musical fifth, or seven semitones, above E♭3. This waterfall plot shows only six strong harmonics, with three that are particularly prominent.

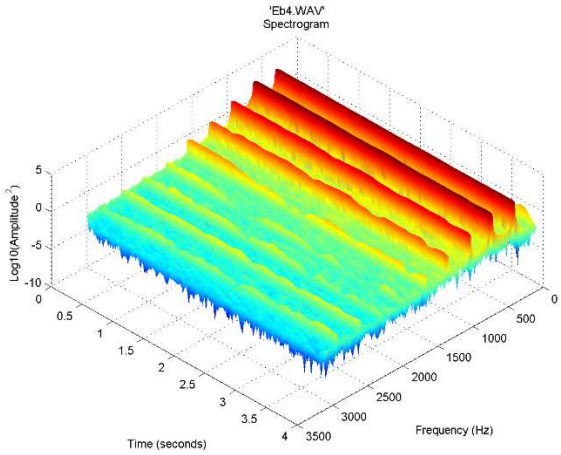

Figure 8 E♭4 is one octave, or 12 semitones, above E♭3. This note shows only four strong harmonics, and to the listener it sounded darker than both B♭3 and E♭3.

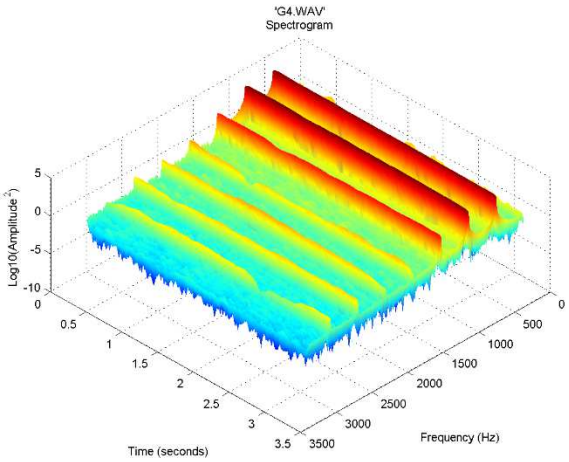

Figure 9 G4 is four semitones above E♭3 and exhibits three strong harmonics.

Figures 10-15 show MATLAB-produced phasor diagrams and harmonic amplitude graphs of notes played on the Alto Horn. In each phasor diagram, the fundamental frequency is denoted by a blue vector at 0°, and the length R of the phasor describes the mean normalized amplitude of each harmonic, where the fundamental is set to 12dB.

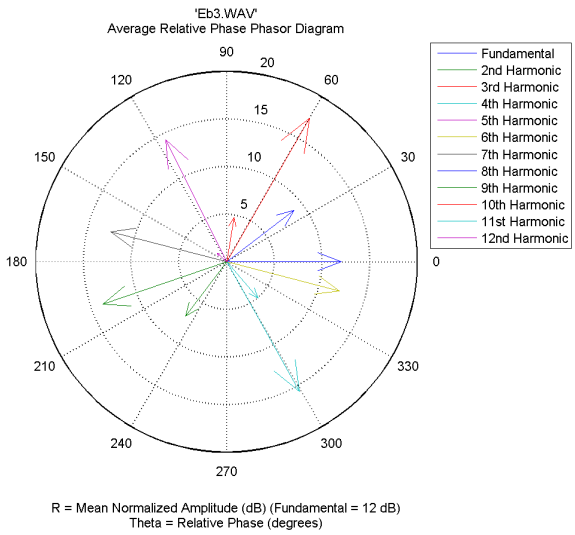

Figure 10 shows the relative phasor diagram of E♭3. Harmonics 3&10, like 4&11, seem to be within ten degrees of one another.

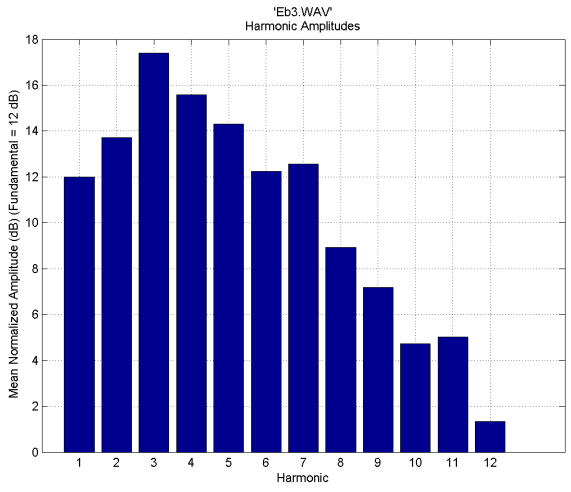

Figure 11 shows the time-averaged amplitude of each harmonic when the note E♭3 was played. The fundamental has a lower amplitude than the second through seventh harmonics.

In order to have resonances, the sound waves must produce standing waves within the air column, meaning that the sound waves must reflect at the bell and return to interfere constructively at the mouthpiece. This happens simultaneously for every resonance. The average relative phasor and amplitude diagrams, then also describe how a player's lips must buzz.

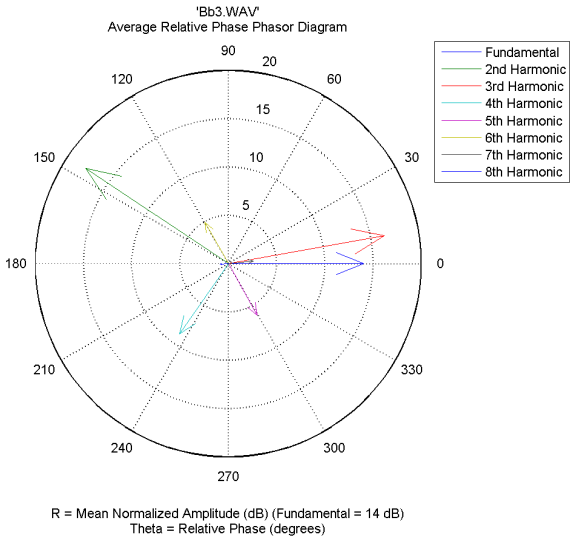

Figure 12 shows the relative phasor diagram for B♭3. Though it is very hard to see, the 8th harmonic is 180° out-of-phase with the fundamental.

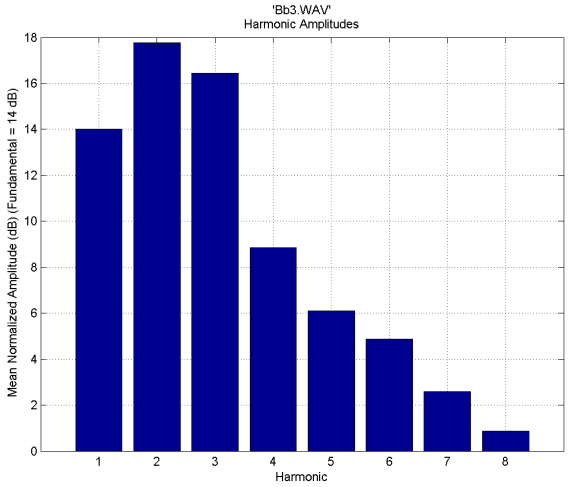

Figure 13 shows the time-averaged amplitude of each harmonic when the note B♭3 was played. The fundamental has a lower amplitude than the second and third harmonics.

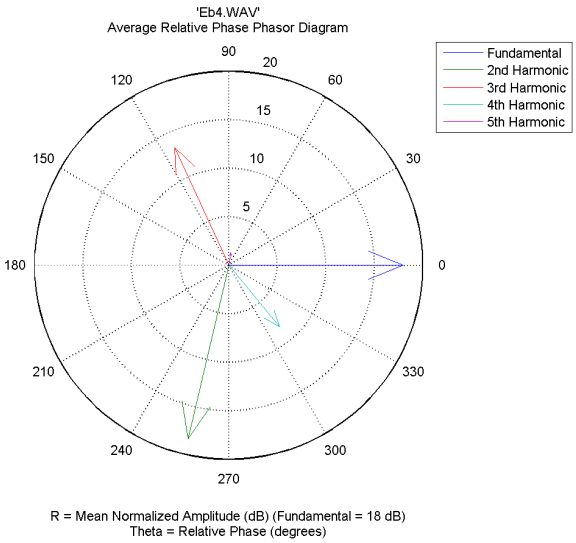

Figure 14 shows the relative phasor diagram for E♭4. The first, second, and third harmonics are nearly 120° in separation.

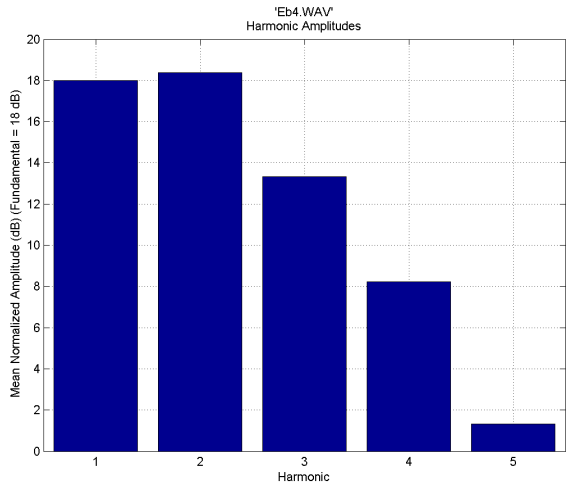

Figure 15 shows the time-averaged amplitude of each harmonic when the note E♭4 was played. The fundamental has a lower amplitude than only the second harmonic.

2. The Euphonium

The harmonic content in the Euphonium was recorded using: first, an SM4M Denis Wick metal mouthpiece, and second with a 5G Kelly plastic mouthpiece, both shown in Figure 16. The Denis Wick mouthpiece has a deeper cup than the Kelly mouthpiece, and is made from a much harder material; these factors play greatly into the harmonic richness of a note, as can be seen in Figures 17 and 18.

Figure 16 shows the Denis Wick SM4M metal mouthpiece on the left, and the clear plastic Kelly 5G mouthpiece on the right.

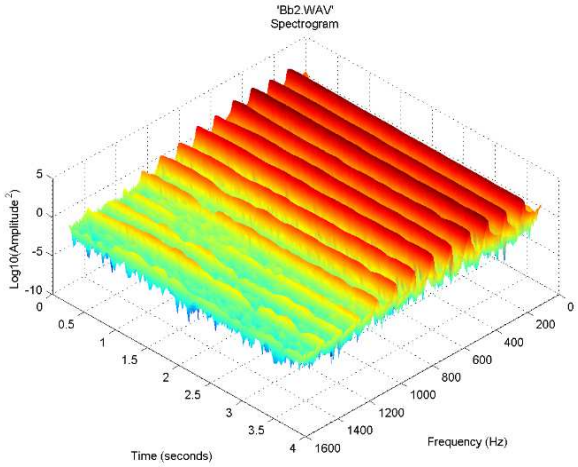

Figure 17 shows the harmonic structure of B♭2 on the Denis Wick metal mouthpiece. The harmonics here are strong out to about 800Hz.

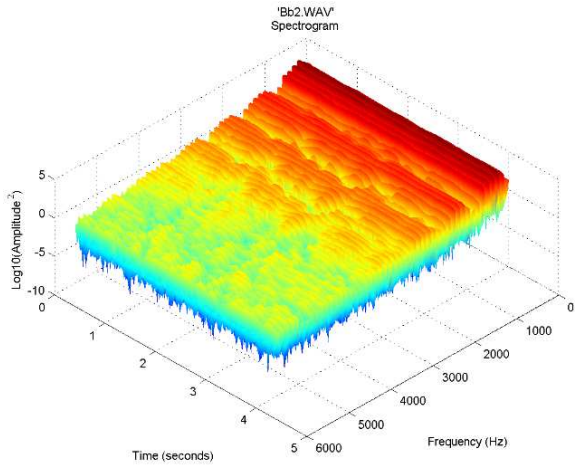

Figure 18 shows the harmonic structure of B♭2 on the Kelly 5G plastic mouthpiece. This mouthpiece excites over twice as many harmonics as the Denis Wick mouthpiece; the harmonics are strong out to 2000Hz.

Like the Alto Horn, the Euphonium's timbre becomes darker as the frequency of the sounded note becomes higher. This is shown in Figures 19-20. The higher harmonics fall off in amplitude as the output impedance at the bell end nears an impedance match, as a standing wave cannot be sustained without wave reflection at the bell end[6].

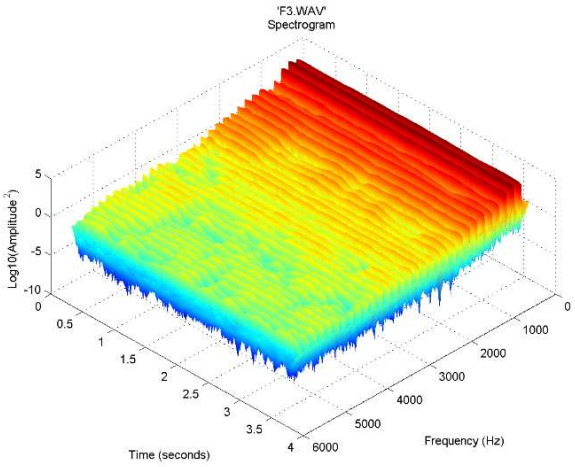

Figure 19 shows the harmonic structure of F_3 as played on the Kelly 5G mouthpiece. There are nine strong harmonics and as many weak ones, all occurring under 3000Hz.

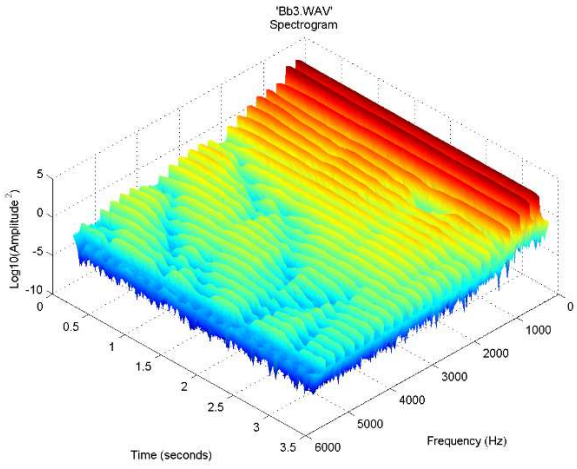

Figure 20 shows the harmonic structure of $B\flat_3$ played on the Kelly 5G mouthpiece. This note is a musical 4th, or five semitones, above F_3 and excites half the harmonics that F_3 does. There are four strong harmonics, with six weaker ones, all below 2000Hz.

The note D_4 was played with two fingerings: open (no valves depressed), and 1+2 (first and second valves depressed). The phase information gathered here shows a potential correlation between phase and tuning. The positioning of the second and third harmonics for open D_4 lead those of 1+2 D_4, as seen in Figures 21 and 22.

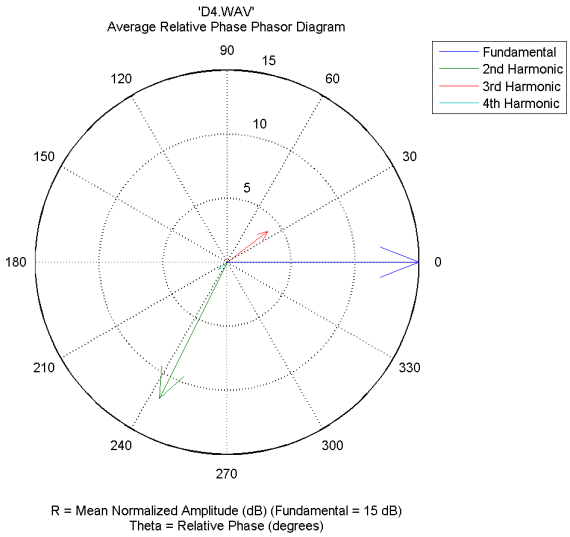

Figure 21 shows the relative phasor diagram of D_4 as played with no valves depressed.

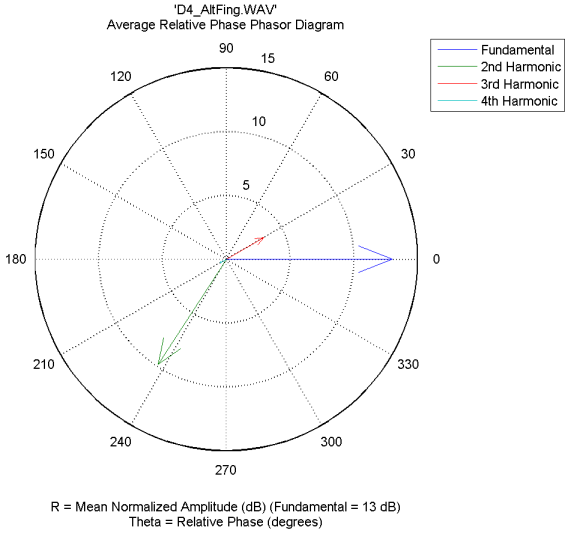

Figure 22 shows the relative phasor diagram of D_4 as played with the first and second valves depressed. It is seen that the second and third harmonics lag those of the note played with no valves depressed.

The instrument's fundamental pitch, B♭1, was played using the Kelly 5G mouthpiece. It was already seen that the lowest pitches were brighter in timbre, but this recording of B♭1 shows that the fundamental pitch itself has an extremely small amplitude relative to its harmonics.

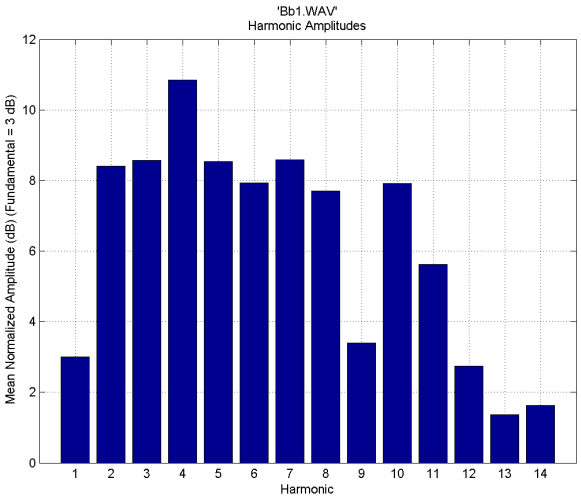

Figure 23 shows the mean normalized harmonic amplitudes of the note B♭1. Where in other notes the fundamental is only slightly weaker than the second through fourth harmonics, in B♭1 the fundamental is at least 5dB weaker than its following harmonics.

Like in the Alto Horn, standing waves in the Euphonium occur at resonant frequencies. The phase diagrams and harmonic amplitude graphs indicate that a player's lips must be buzzing at each of these frequencies. Each sound wave produced by the lips has phase and amplitude as shown by the data as represented in Figures 24-29.

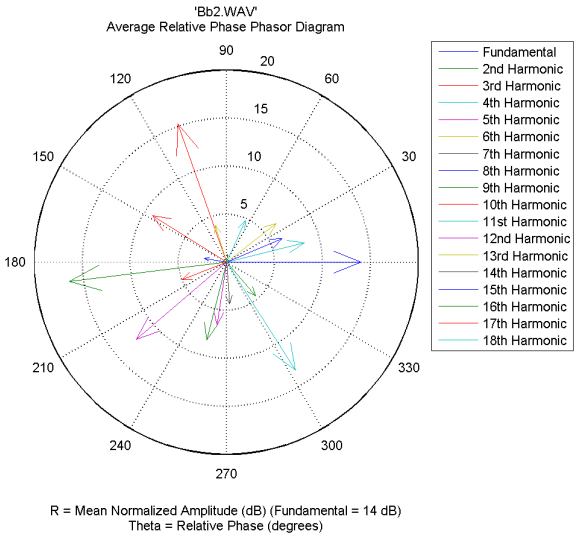

Figure 24 shows the relative phasor diagram of B♭2. The arising pattern here is that groups of harmonics: the 3rd, 10th, and 17th; the 2nd, 9th, and 16th, seem to be grouped 45° from one another.

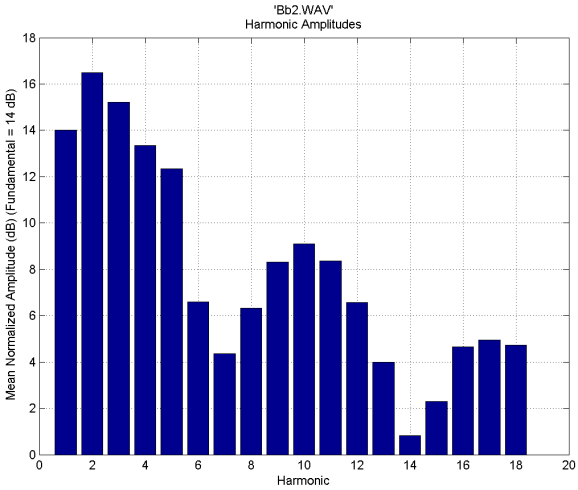

Figure 25 shows the mean normalized harmonic amplitudes of the note B♭2. This diagram shows three batches of strong harmonics, with dips at the seventh and 14th harmonics.

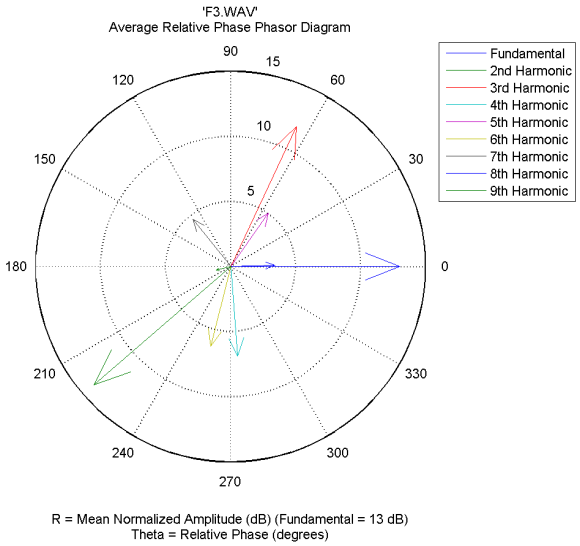

Figure 26 shows the relative phasor diagram of F3, which is seven semitones above B♭2. In this case, the fundamental and 8th harmonic are nearly in-phase.

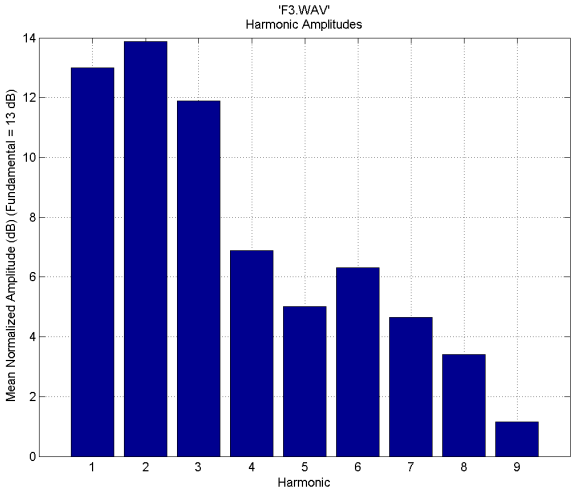

Figure 27 shows the mean normalized harmonic amplitudes of the note F3. The second harmonic is approximately 1dB higher in amplitude than the fundamental, and though there is variation in the higher harmonics (5-8), the batch pattern as in Figure 25 is not seen here.

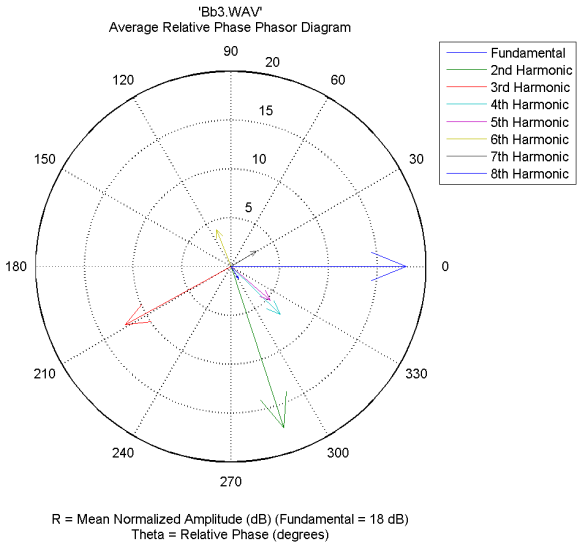

Figure 28 shows the relative phasor diagram of B♭3. The fourth and fifth harmonics are nearly in-phase, while the second and third harmonics are nearly 90° out-of-phase.

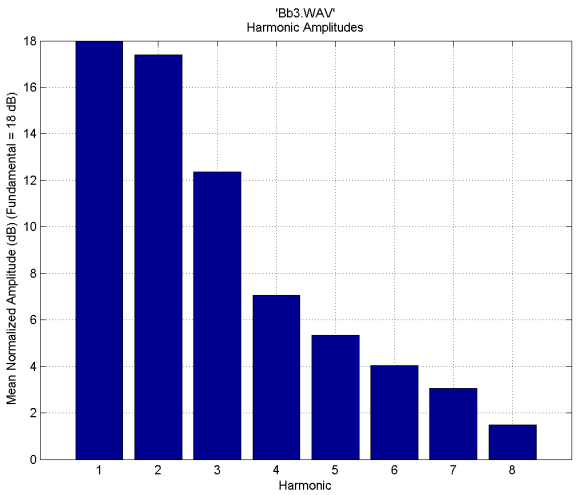

Figure 29 shows the mean normalized harmonic amplitudes of the note B♭3. Here, the fundamental is strongest, with a strong second harmonic but a nearly linear drop off in amplitude after the third harmonic.

B. Frequency Scan

The harmonic analysis shows what approximate range of frequencies should be scanned to determine exact resonances. Both the Alto Horn and Euphonium were tested to find the resonances of the instrument with no valves depressed.

Resonant frequencies are calculated by finding the maximum input impedance, $\tilde{z}$, where the pressure is near a maximum and the particle velocity is near a minimum. Figures 30 and 32 show the input impedance peaks, and therefore resonant frequencies, for the Alto Horn and Euphonium respectively. Figures 31 and 33 show the output impedance curves. Paired, these graphs show that when the output impedance at the bell approaches the impedance of free air, the resonant peaks are significantly less pronounced.

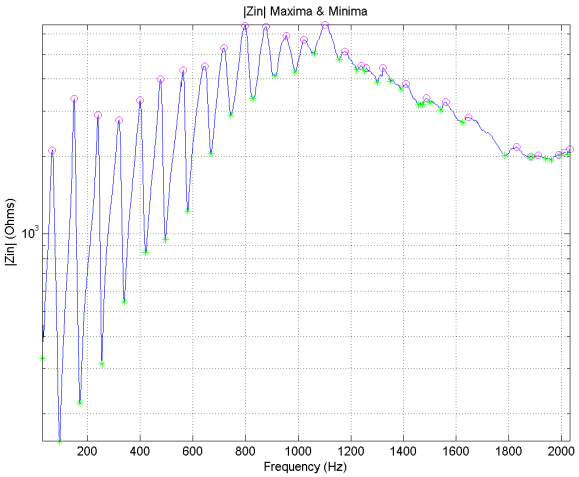

Figure 30 shows the $|\tilde{Z}_{in}|$ resonance curve for the Alto Horn. The pink circles indicate maxima $|\tilde{Z}|$ and therefore the frequency of playable notes. Green stars indicate impedance minima.

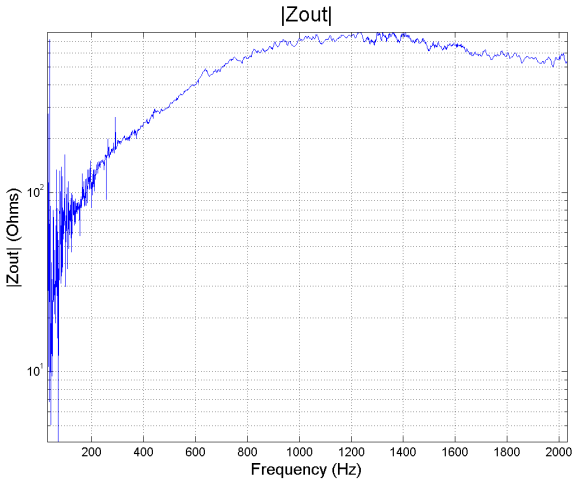

Figure 31 shows the $|\tilde{Z}_{out}|$ curve for the Alto Horn.

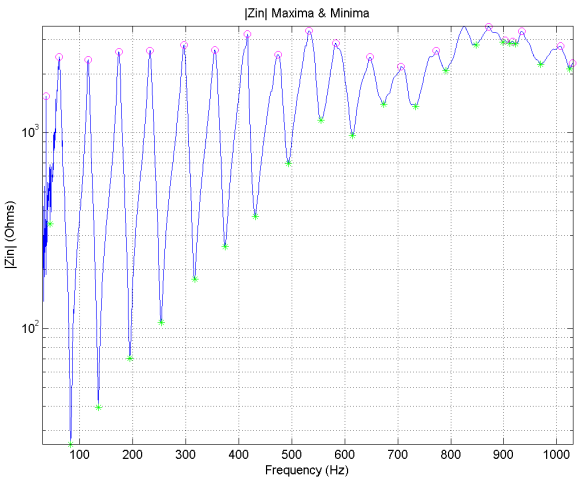

Figure 32 shows the $|\tilde{Z}_{in}|$ resonance curve for the Euphonium. The pink circles indicate maxima $|\tilde{Z}|$ and therefore the frequency of playable notes. Green stars indicate impedance minima.

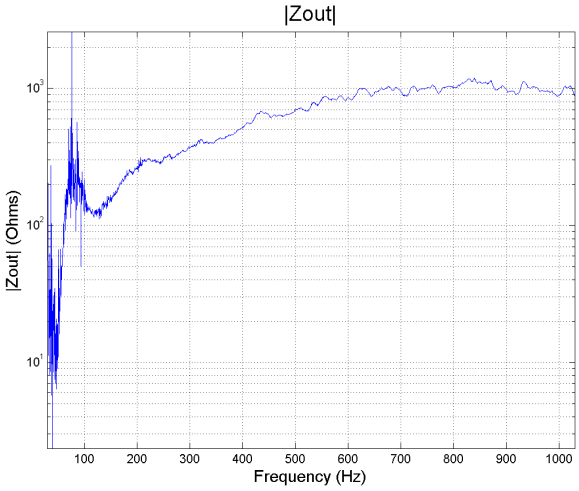

Figure 22 shows the $|\tilde{Z}_{out}|$ curve for the Euphonium.

Resonances must have a high amplitude to be playable; their peak height determines the stability of the note and its ease of play[8]. It can be seen above in Figures 30 and 32 that resonance peaks become wider as the frequency increases. When the output impedance of the bell matches the input impedance of the system, there will be no reflection of sound waves, and the notes will become unplayable.

C. XY-Planar Scans

The values of the resonant frequencies determined which frequencies were used in the XY-planar scans. These scans show that pressure and particle velocity are not constant across the area of the bell, as seen in Figures 26 and 27. As the frequency increases, the rate at which $\tilde{p}$ and $\tilde{u}$ fall off increases due to sound wave diffraction at the bell.

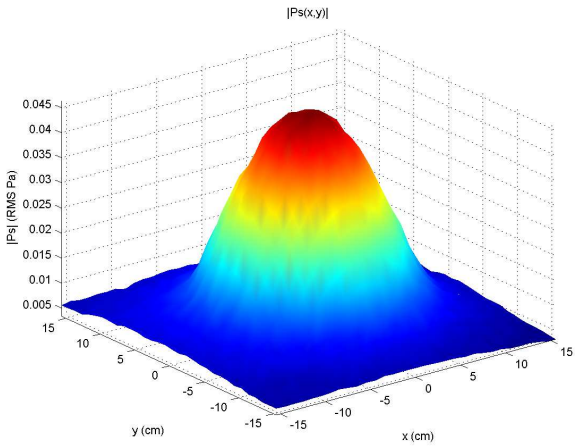

Figure 26 shows the magnitude of pressure across the bell of the Alto Horn when its air column is excited at 398Hz.

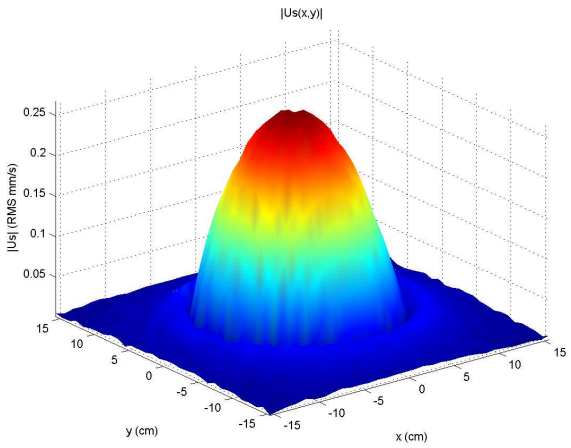

Figure 27 shows the magnitude of particle velocity across the bell of the Alto Horn when its air column is excited at 398Hz. The particle velocity dips as the waves curl around the edge of the bell, accounting for the apparent ring at the base of the form in this graph.

At alternating integer resonant frequencies, the real and imaginary parts of complex pressure and particle velocity at the bell end switched sign. The phase of these quantities also flipped 180° at each consecutive resonance. This phenomenon occurred with both instruments.

The scans show that the phase of each value across the bell is approximately constant, as seen in Figures 28-31. This illustrates the planar nature of sound waves in an air column at the bell.

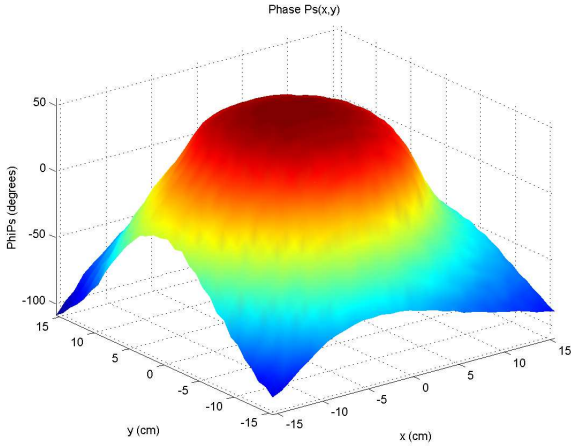

Figure 28 shows the phase of the pressure at the bell end as scanned on the Alto Horn at 700Hz. It is nearly constant across the bell and curves gently out toward the boundaries of the scan.

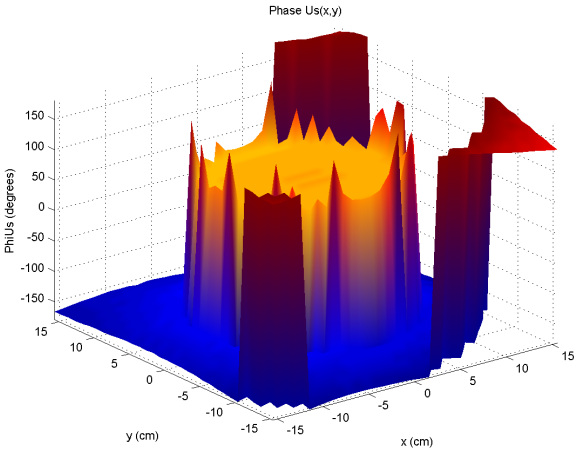

Figure 29 shows the phase of the particle velocity at the bell end as scanned on the Alto Horn at 700Hz. It is nearly constant across the bell but shows a great drop off at the edge of the bell.

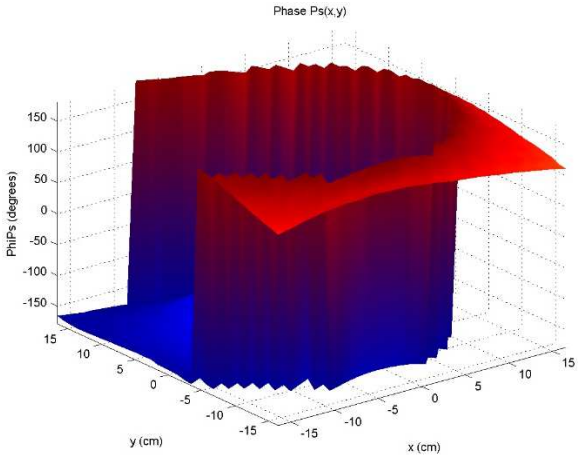

Figure 30 shows the phase of the pressure at the bell end as scanned on the Euphonium at 700Hz. Toward the origin of the plot, the graph shows a curvature similar to that in Figure 28.

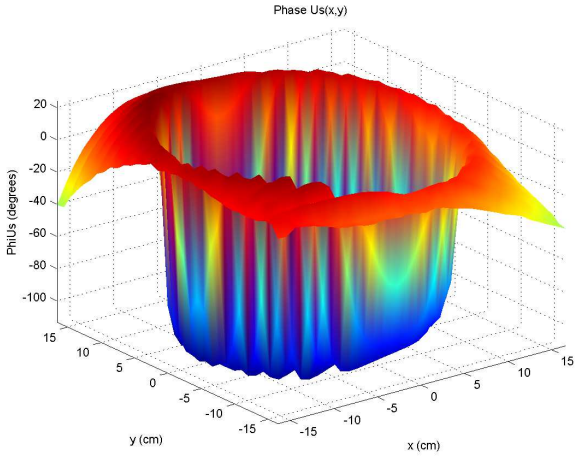

Figure 31 shows the phase of the particle velocity at the bell end as scanned on the Euphonium at 700Hz.

D. Circuit Model

For the Alto Horn, the ratio of areas between the bell and the back bore of the mouthpiece was calculated to be approximately 413:1. Using average $\tilde{p}$, $\tilde{u}$, and $\tilde{z}$ across the bell, the circuit was solved to predict a resonance of 239Hz. This prediction is close to the measured resonance value of f_3 = 240.5Hz.

The product LC was calculated using the experimental function generator frequency. Figures 32 and 33 show the developed circuit with an AC Analysis.

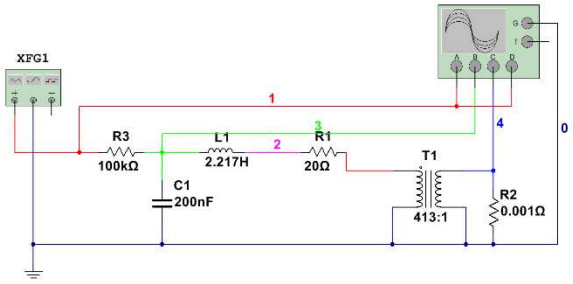

Figure 32 shows the developed circuit analog for the acoustical system of the CG Conn Alto Horn. A function generator drives the system, which is composed of an input resistor, a capacitor, a series inductance and resistance, a transformer, and a load resistance.

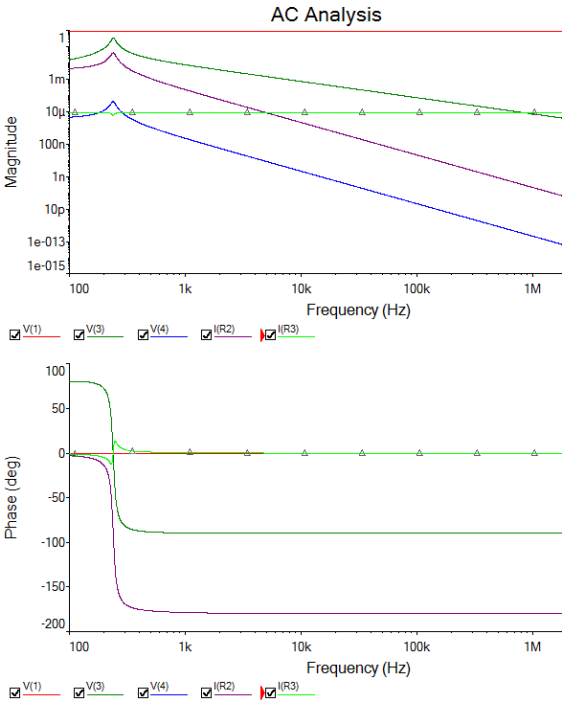

Figure 33 shows an AC analysis performed on the developed circuit with a resonance at 238.6Hz.

In the model, simulation predicted the correct frequency. It is a lumped-parameter model, while the elements of the real acoustic circuit are spatially distributed in nature. In future work, separate L and C calculations should be determined experimentally, and a distributed model should be constructed.

IV. Conclusions

This investigation has identified some reasoning behind musicians' definition of "bright" and "dark" timbre across the range of the instrument. As the harmonic analysis shows, the lowest notes played on a euphonium or alto horn are the richest in harmonics, correlating to a brighter sound. This correlation could be continued in testing of tubas, trombones, trumpets, and French horns.

The observed phasor pattern of harmonics shows that the lips must vibrate at multiple frequencies and phases to produce each note.

Data from the XY-planar scans show that pressure and particle velocity are only approximately constant across the cross-sectional surface area of the bell, and that there is a 180° phase shift between even- and odd- integer harmonics. Both phenomena should be investigated further with testing of other low brass instruments and theoretical models.

Other potential future work includes: improving the electrical circuit model; overlaying data from XY-planar scans to characterize the air column as excited by superposition of multiple harmonics; modelling the instruments as a set of acoustic 'horns' that are linearly combined using a least-squares fit test.

V. Acknowledgements

I would like to thank Dr. Errede for his guidance in this project and for allowing me the use of his sensitive laboratory equipment. I would also like to acknowledge Jack Bopari for his assistance in equipment acquisition, and Patrick Barry for his discussion and conceptual assistance.

The REU program is supported by NSF Grant PHY-1062690.

VI. References

[1] "Euphonium." Origin. *Merriam-Webster*. n.d. N. pag. Web. 15 June 2014. <http://www.merriam-webster.com/dictionary/euphonium>.

[2] S. Errede, "Consonance and Dissonance," (2002-2014) (unpublished). <https://courses.physics.illinois.edu/phys406/Lecture_Notes/P406POM_Lecture_Notes/P406POM_Lect8.pdf>

[3] NH Fletcher, TD Rossing, *The Physics of Musical Instruments,* 2nd Edition. (1998), pp.434

[4] J. Yasi, "An Algorithm for Extracting the Relative Phase of Harmonics from a Periodic Digital Signal," (2004) (unpublished). <http://courses.physics.illinois.edu/phys406/NSF_REU_Reports/2004_reu/Joe_Yasi_Final_Paper.pdf>

[5] B. Sullivan, "Near-Field Acoustic Holography of a Vibrating Drum Head," (2008) (unpublished). <https://courses.physics.illinois.edu/phys406/NSF_REU_Reports/2008_reu/Brendan_Sullivan_Senior_Thesis/bsullivan_senior_thesis.pdf>

[6] D. Pignotti, "Acoustic Impedance of a Bb Trumpet," 8-20 (2008) (unpublished). <https://courses.physics.illinois.edu/phys406/NSF_REU_Reports/2007_reu/David_Pignotti_Senior_Thesis/David_Pignotti_Senior_Thesis.pdf>

[7] N. D'Anna, "Data Acquisition with the PXIe-4492," (2013) (unpublished). <https://courses.physics.illinois.edu/phys406/Student_Projects/Spring13/Nick_DAnna_P406_Final_Project_Report_Sp13.pdf

[8] A. Watts, "Spectral Analysis of the French Horn and the Hand-in-Bell Effect," 5 (2009) (unpublished). <https://courses.physics.illinois.edu/phys406/NSF_REU_Reports/2009_reu/Adam_Watts/adamwatts_thesis.pdf>